NREL/TP-413-5092 • UC Category: 273 • DE92016444

Development of a Computer Model for Polycrystalline Thin-Film $CuInSe_2$ and CdTe Solar Cells

Final Subcontract Report
1 January 1991 – 31 December 1991

NREL/TP--413-5092

DE92 016444

J. L. Gray, R. J. Schwartz, Y. J. Lee
Purdue University
West Lafayette, Indiana

NREL technical monitor: H. S. Ullal

National Renewable Energy Laboratory
1617 Cole Boulevard
Golden, Colorado 80401-3393
A Division of Midwest Research Institute
Operated for the U.S. Department of Energy
under Contract No. DE-AC02-83CH10093

Prepared under Subcontract No. XN-0-10013-1

September 1992

MASTER

DISTRIBUTION OF THIS DOCUMENT IS UNLIMITED

On September 16, 1991 the Solar Energy Institute was designated a national laboratory, and its name was changed to the National Renewable Energy Laboratory.

NOTICE

This report was prepared as an account of work sponsored by an agency of the United States government. Neither the United States government nor any agency thereof, nor any of their employees, makes any warranty, express or implied, or assumes any legal liability or responsibility for the accuracy, completeness, or usefulness of any information, apparatus, product, or process disclosed, or represents that its use would not infringe privately owned rights. Reference herein to any specific commercial product, process, or service by trade name, trademark, manufacturer, or otherwise does not necessarily constitute or imply its endorsement, recommendation, or favoring by the United States government or any agency thereof. The views and opinions of authors expressed herein do not necessarily state or reflect those of the United States government or any agency thereof.

Printed in the United States of America
Available from:
National Technical Information Service
U.S. Department of Commerce
5285 Port Royal Road
Springfield, VA 22161

Price: Microfiche A01
Printed Copy A04

Codes are used for pricing all publications. The code is determined by the number of pages in the publication. Information pertaining to the pricing codes can be found in the current issue of the following publications which are generally available in most libraries: *Energy Research Abstracts (ERA)*; *Government Reports Announcements* and Index (*GRA* and I); *Scientific and Technical Abstract Reports (STAR)*; and publication NTIS-PR-360 available from NTIS at the above address.

DISCLAIMER

Portions of this document may be illegible electronic image products. Images are produced from the best available original document.

Table of Contents

1 Introduction 1
1.1 Project Overview 1
1.2 Outline of Report 1

2 ADEPT 3
2.1 Introduction 3
2.2 Basic Formulation 3
2.2.1 Band Parameters 4
2.2.2 Non-mobile Trapped Charge 5
2.2.3 Recombination 5
2.2.4 Generation 6
2.3 Numerical Solution 6
2.4 Device Analyses 7

3 Summary and Recommendations 9

4 References 11

Appendix A 13

Appendix B 19

Appendix C 25

Appendix D 31

1 Introduction

1.1 Project Overview

A primary objective of this research was to develop an accurate numerical model for $CuInSe_2$ (CIS) and CdTe based solar cells capable of running on a personal computer. Such a model will aid researchers in the design and analysis of CIS and CdTe based solar cells. ADEPT (A Device Emulation Program and Tool) was used as the basis for this model. An additional objective of this research was to use the models developed here to analyze the performance of existing and proposed CIS and CdTe based solar cells.

The development of accurate numerical models for CIS and CdTe based solar cells required the compilation of cell performance data (for use in model verification) and the compilation of measurements of material parameters. Each of these is an ongoing task, so that the models can reflect the best available information. The first year of this project focused primarily on these tasks. The results of the initial compilation of information is available in [1].

The development of the numerical models involved implementing the various physical models appropriate to CIS and CdTe, as well as some common window materials. Many parameters needed in these models are not well known, and therefore the numerical model must be used to determine reasonable choices and the choice of these parameters must be periodically examined as new information (i.e. cell and material measurements) is made available. In addition, a version of the model capable of running on a IBM compatible personal computer was developed (primary code development is on a SUN workstation) so that the model can be more widely distributed. Finally, a user friendly interface with pop-up menus is continuing to be developed for release with the IBM compatible model.

1.2 Outline of Report

Chapter 2 of this report gives an overview of the general device simulation model, ADEPT with emphasis on those aspects of the code relevant to CIS and CdTe based solar cells. Chapter 3 gives a summary of results to date as well as recommendations for future work. Appendices A, B, and C are copies of papers detailing some of the results of this research [2-4]. These papers were presented at the 22nd IEEE Photovoltaic Specialists Conference in Las Vegas, Nevada during October 1991 and will appear in the proceedings of this conference. In Appendix D, the user's guide for ADEPT/F (1D Fortran version) for IBM compatibles is included.

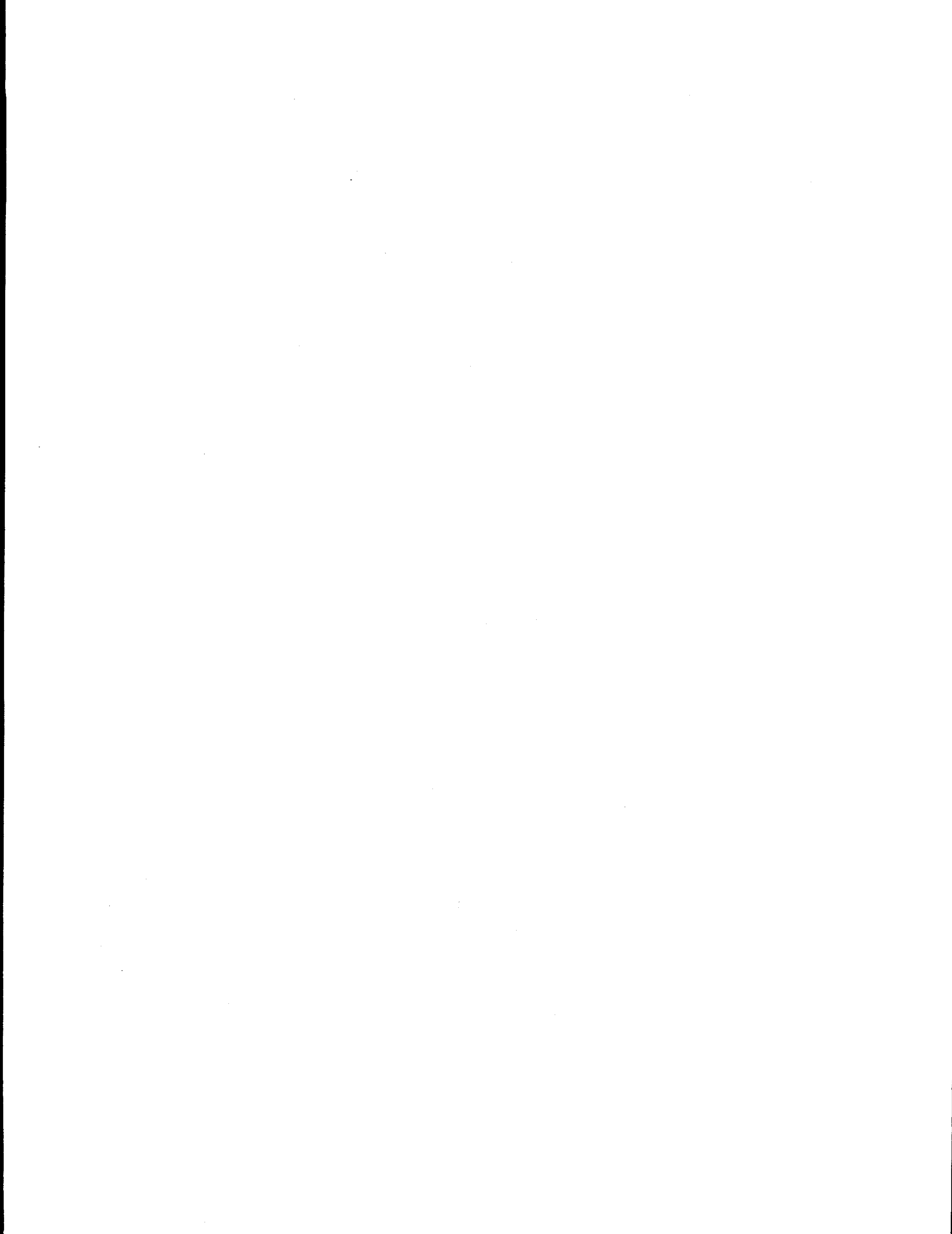

2 ADEPT

2.1 Introduction

The purpose of this chapter is to give potential users of the numerical model developed during this contract (ADEPT/1D for CIS & CdTe Solar Cells) a basic understanding of the model and its basis.

ADEPT is being developed to be a general purpose computer model capable of modeling a wide variety of devices and materials in one, two, or three spatial dimensions. It can be modified by an experienced user to include new material models and new device analyses - thus making it a flexible and convenient research tool. The emphasis here will be on aspects of the numerical model that are of significance to modeling CIS and CdTe based solar cells in one-dimension. Many of these features are also described in [5].

2.2 Basic Formulation

Both CIS and CdTe based solar cells have basically one-dimensional structures. Thus, a 1D model (which can be run on a PC) is sufficient to model these cells. Detailed investigation of grain boundary effects, however, will necessitate the use of 2D and/or 3D models. These issues will be addressed in future work.

The operation of many semiconductor devices, including CIS and CdTe solar cells, can be described by the solution of the three semiconductor equations - Poisson's equation and the hole & electron continuity equations. These three coupled nonlinear partial differential equations are shown below for steady-state, isothermal conditions.

$$\vec{\nabla} \cdot \vec{D} = \rho$$

$$\vec{\nabla} \cdot \vec{J}_p = q\,(G - R)$$

$$\vec{\nabla} \cdot \vec{J}_n = q\,(R - G)$$

In the above equations, $\vec{D}$ is the displacement field, ρ is the charge density, $\vec{J}_p$ & $\vec{J}_n$ are the current densities, G is the generation rate, and R is the recombination rate. The unknowns that are to be solved for are the electrostatic potential, V, and the hole & electron carrier concentrations, p & n. The unknowns appear explicitly in the following auxiliary equations.

$$\vec{D} = \varepsilon\vec{E} = -\varepsilon\vec{\nabla}V$$

$$\rho = q(p - n + N)$$

$$\vec{J}_p = -q\mu_p p \vec{\nabla}(V - V_p) - qD_p \vec{\nabla} p$$

$$\vec{J}_n = -q\mu_n n \vec{\nabla}(V + V_n) + qD_n \vec{\nabla} n$$

Here, ε is the position dependent electric permittivity of the semiconductor, $\vec{E}$ is the electric field, N is the non-mobile trapped charge, μ_p & μ_n and D_p & D_n are the mobilities and diffusion coefficients of holes & electrons, respectively, and V_p & V_n are the so-called band parameters.

It should be noted that the solution of these equations describe all aspects of device operation from contact to contact (assuming that the pertinent physics has been properly modeled). Thus, effects such as collection losses due to back diffusion and junction recombination are automatically accounted for.

ADEPT's versatility stems from the fact that this basic formulation will apply to almost any semiconductor material. The specific physical properties of the semiconductor are contained in the following terms: ε, N, μ_p, μ_n, D_p, D_n, V_p, V_n, and G, and R. Therefore, to model a specific material, one must develop appropriate models for these parameters.

Some of these (ε, μ_p, μ_n, D_p, and D_n) can be inferred directly from appropriate measurements. At present, no explicit field, temperature, or carrier density dependencies for the preceding parameters are modeled in ADEPT. However, the user does have direct access to these parameters and can include these dependencies in an *ad hoc* manner. Also, such dependencies will be included explicitly in future releases.

The others parameters are more complicated and will be discussed further in the following subsections.

2.2.1 Band Parameters

The band parameters are terms which account for position dependent electron affinity, position dependent bandgap, position dependent conduction band and valence band densities-of-state, and Fermi-Dirac statistics. In is these terms that make it possible for ADEPT to model heterostructures. This is necessary when modeling CIS and CdTe based solar cells since these devices are typically fabricated with wide bandgap window layers such as CdS.

Values for the electron affinity, χ, the bandgap, E_G, and the conduction and valence band densities-of-state, N_C and N_V, must be provided to ADEPT. Unfortunately, there is some uncertainty as to the correct values of these parameters in CIS, CdTe, and CdS, and the user must carefully choose appropriate values.

2.2.2 Non-mobile Trapped Charge

The non-mobile trapped charge, N, is used to model midgap defects that arise due to an imperfect crystal structure and/or impurities. ADEPT supports a number of possible defect types (see [5]). The simplest approach is to set a fixed amount of trapped charge so that the observed majority carrier concentration is created. This has been the initial approach in our modeling of CIS and CdTe based solar cells. However, there are a number of known defect levels that are thought to control the self doping of these materials, and ADEPT can be used to investigate these defects.

In order to model these levels, it is necessary to know their concentration, their capture coefficients, their location (in energy), and their character (i.e. donor-like, acceptor-like, multiply ionized, etc.). Thus far, no specific recommendations as to the proper choice of this parameters can be made. This is left to future investigations.

2.2.3 Recombination

The defects discussed in the previous section can all act as recombination sites and models for recombination via each of these defects have been implemented in ADEPT. However, as stated before, no specific recommendations can as yet be made as to the proper model to use. Our initial approach has been to model recombination as a simple Shockley-Hall-Read process by specifying appropriate carrier lifetimes. This simple approach has helped in developing a basic understanding of cell operation, but a more rigorous approach will be necessary in order to develop a complete picture of CIS and CdTe based solar cell performance.

ADEPT can also model other basic recombination mechanisms, such as direct band-to-band recombination and Auger recombination, so long as appropriate values of the respective coefficients are known.

2.2.4 Generation

While there are other potential sources of carrier generation (i.e. impact ionization), in solar cells the most important source of carrier generation is optical generation. Models for optical absorption in CIS, CdTe, and CdS have been developed and ADEPT can model the optical generation of carriers due to a variety of incident solar spectra. Effects such as reflection, light trapping, and grid shadowing can be modeled as well.

2.3 Numerical Solution

As was seen in the previous section, the operation of a solar cell can be described by the solution of three coupled nonlinear partial differential equations. These equations cannot be solved analytically, except under specific simplified conditions. It is therefore necessary to resort to a numerical solution.

The first step in obtaining a numerical solution is to discretize the differential equations to obtain difference equations. In ADEPT, this is accomplished by defining a mesh on which, at each node, the differential equations are discretized. Thus, three difference equations are obtained at each node, resulting a set of 3N coupled nonlinear difference equations, where N is the number of nodes in the mesh. Typically, from 200 to 250 nodes are used. ADEPT can automatically create this mesh. This is accomplished by examining the approximations that were used to discretize the equations and selecting node positions such that the restrictions imposed by these approximations are satisfied.

This nonlinear set of equations can be represented as follows.

$$\overline{F}(\overline{p},\overline{n},\overline{V}) = 0$$

where $\overline{p}$, $\overline{n}$, and $\overline{V}$ are vectors of the unknowns evaluated at each node.

A generalization of Newton's method is then used to obtain a solution. This is shown below for the $(k+1)^{st}$ Newton iteration.

$$J^k \Delta U^{k+1} = -\overline{F}^k$$

$$\overline{U}^{k+1} = \overline{U}^k + \Delta\overline{U}^{k+1}$$

Here $\overline{U}$ is the combined vector of length 3N containing $\overline{p}$, $\overline{n}$, and $\overline{V}$. The iteration continues until the correction vector is small enough to neglect. This typically occurs in fewer than 10 Newton iterations. The Jacobi matrix, J^k, is obtained by taking the partial derivative of each difference equation at each node with respect to each unknown on the entire mesh, creating a 3N by 3N matrix. Therefore, each Newton iteration requires the solution of a matrix equation of order 3N. Fortunately, the Jacobi matrix is sparse and banded. In one-dimension, the bandwidth is typically nine. A special numerical algorithm for solving banded matrix equations is used, and can be run quite easily on a personal computer.

2.4 Device Analyses

Any experiment that can be performed in the laboratory can be simulated as well. This permits model verification and provides feedback for researchers in interpreting the experiments. Confidence in the model is merited if a single set of model parameters fits a wide range of experiments, such as light IV, dark IV, spectral response, and photoconductivity, to name a few. ADEPT is set up to make the addition of new analyses quick and easy.

Simulation also offers the researcher the ability to appear inside the device and observe the behavior of the internal parameters directly. This ability provides an intuition which is difficult to attain in any other way. Loss mechanisms can be observed directly and design changes can be tested in advance. ADEPT provides access to each internal parameter so that they can be manipulated and examined by the user.

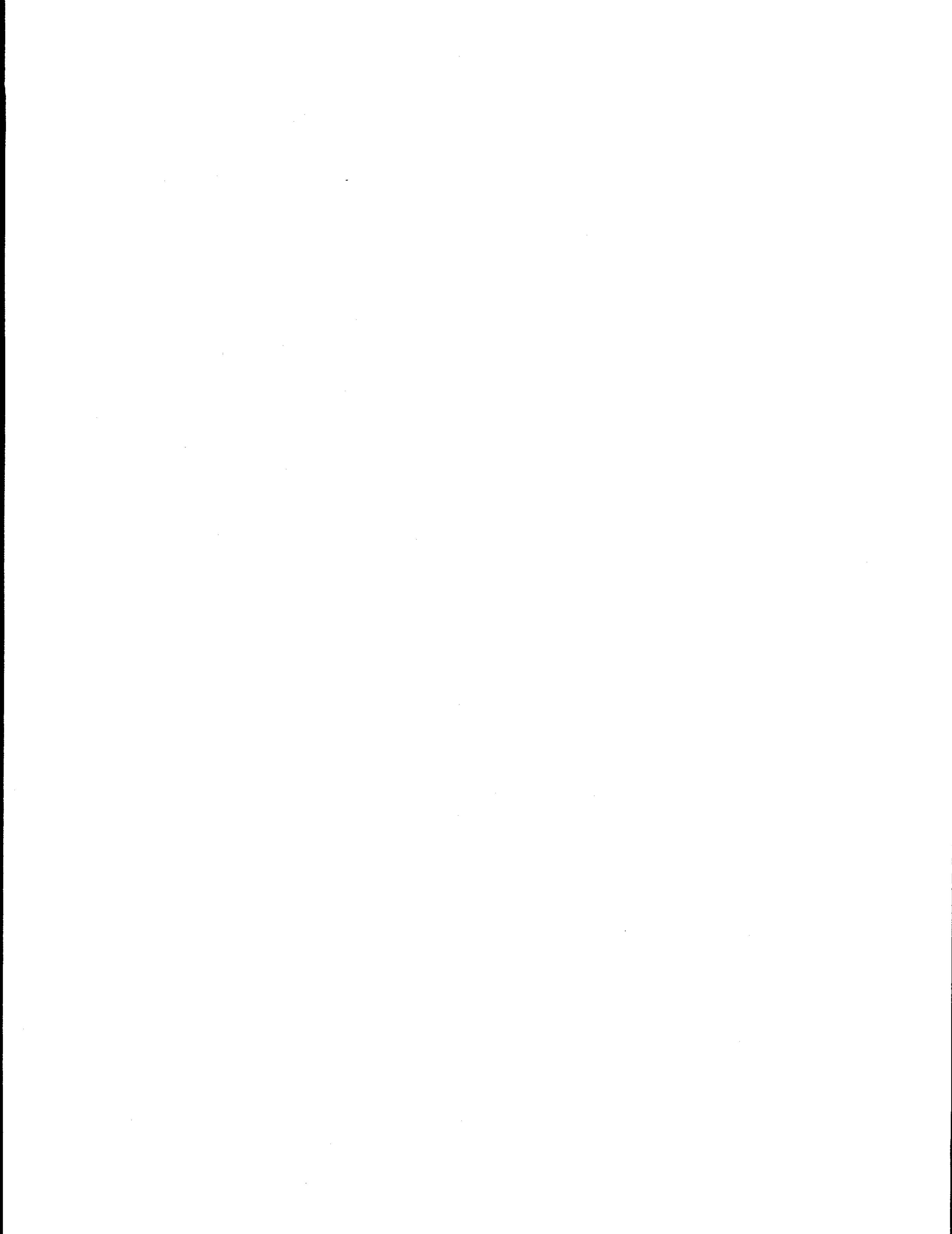

3 Summary and Recommendations

A one-dimensional simulation code, ADEPT, has been developed for the simulation of CIS and CdTe based solar cells has been developed. This code runs on IBM compatible personal computers, as well as Sun workstations. Simple models for carrier generation, recombination, and transport have been developed. ADEPT has been used to examine design constraints for CIS and CdTe based solar cells. However, these materials are still not well understood and additional work is needed to develop better physical models for implementation into ADEPT. For example, the role of defects in determining material type, as well as their role in recombination and transport, must be more carefully examined.

Future work will involve updating model parameters and developing new physical models for implementation into ADEPT. Updated releases of ADEPT for CIS and CdTe based solar cells, for use on IBM compatible personal computers, will be made available to photovoltaic researchers. In addition, ADEPT will be utilized to analyze existing devices, make design recommendations, and make performance predictions.

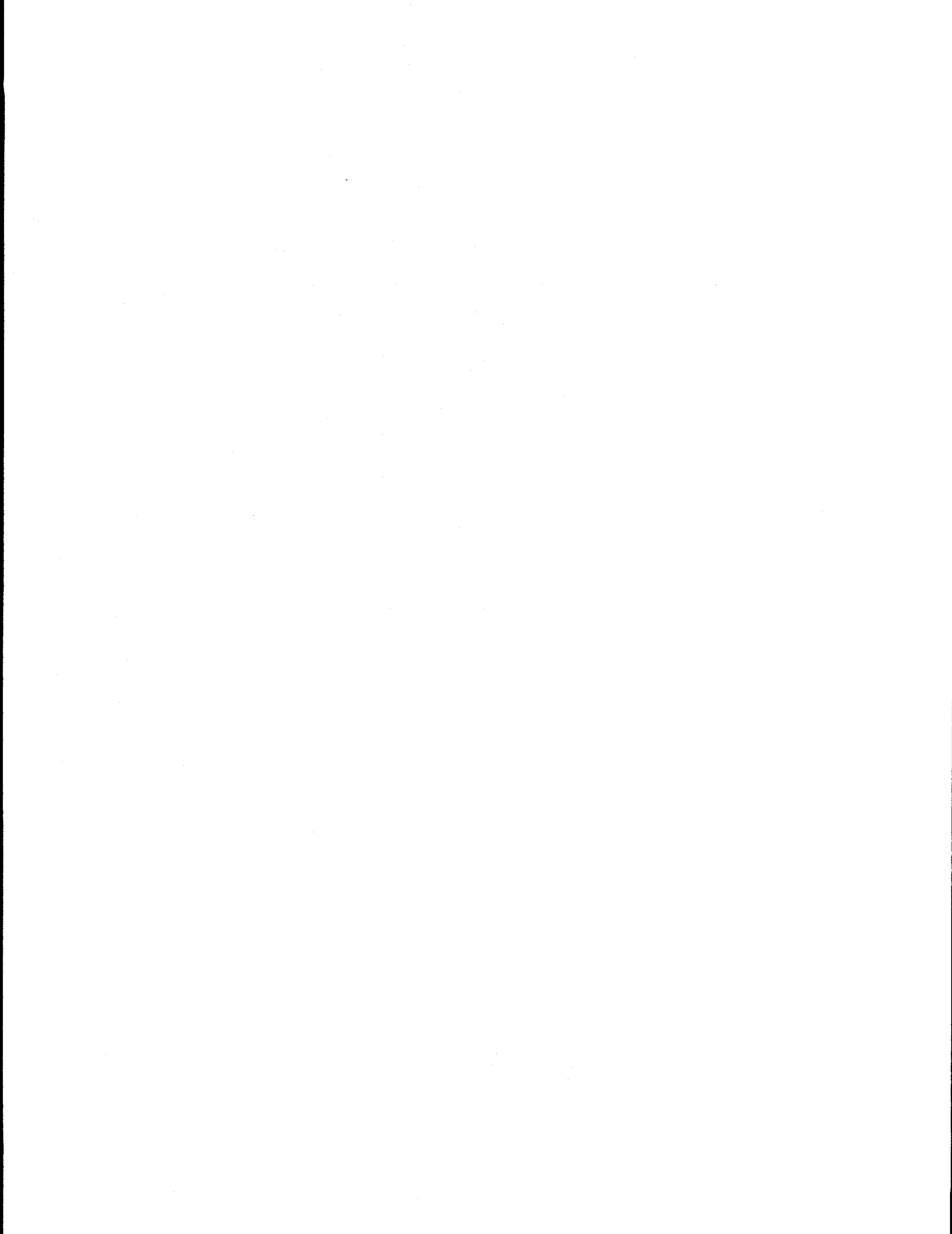

4 References

[1] Jeffery L. Gray, Richard J. Schwartz, and Youn Jung Lee, "Annual Report on the Development of a Computer Model for Polycrystalline Thin-Film $CuInSe_2$ and CdTe Solar Cells," TR-EE 91-49, School of Electrical Engineering, Purdue University, West Lafayette, Indiana, January 1992.

[2] Jeffery L. Gray, "ADEPT: A General Purpose Numerical Device Simulator for Modeling Solar Cells in One-, Two-, and Three-Dimensions," Conference Record of the Twenty-Second IEEE Photovoltaic Specialists Conference in Las Vegas, Nevada, pp. 436-438, October 1991.

[3] Youn Jung Lee and Jeffery L. Gray, "Numerical Modeling of CdS/CdTe Solar Cells: A Parameter Study," Conference Record of the Twenty-Second IEEE Photovoltaic Specialists Conference in Las Vegas, Nevada, pp. 1151-1154, October 1991.

[4] R. J. Schwartz, J. L. Gray, and Y. J. Lee, "Design Considerations for Thin Film $CuInSe_2$ and Other Polycrystalline Heterojunction Solar Cells," Conference Record of the Twenty-Second IEEE Photovoltaic Specialists Conference in Las Vegas, Nevada, pp. 920-923, October 1991.

[5] Jeffery L. Gray, "A Computer Model for the Simulation of Thin-Film Silicon-Hydrogen Alloy Solar Cells," IEEE Transactions on Electron Devices, Vol. 36, No. 5, May 1989.

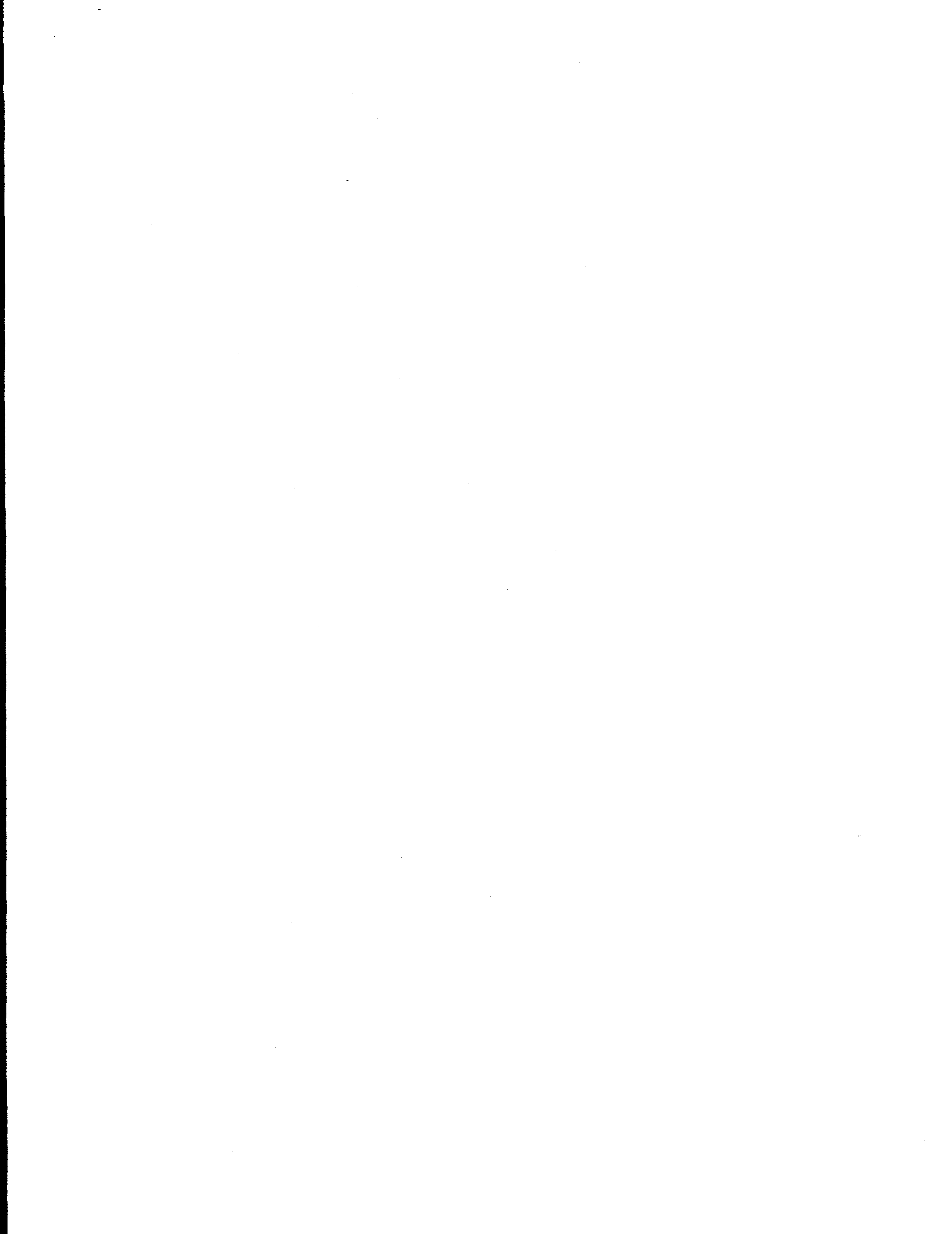

Appendix A

This appendix contains a copy of a paper entitled "ADEPT: A General Purpose Numerical Device Simulator for Modeling Solar Cells in One-, Two-, and Three-Dimensions" that was presented at and appears in the Conference Record of the Twenty-Second IEEE Photovoltaic Specialists Conference in Las Vegas, Nevada, October 1991.

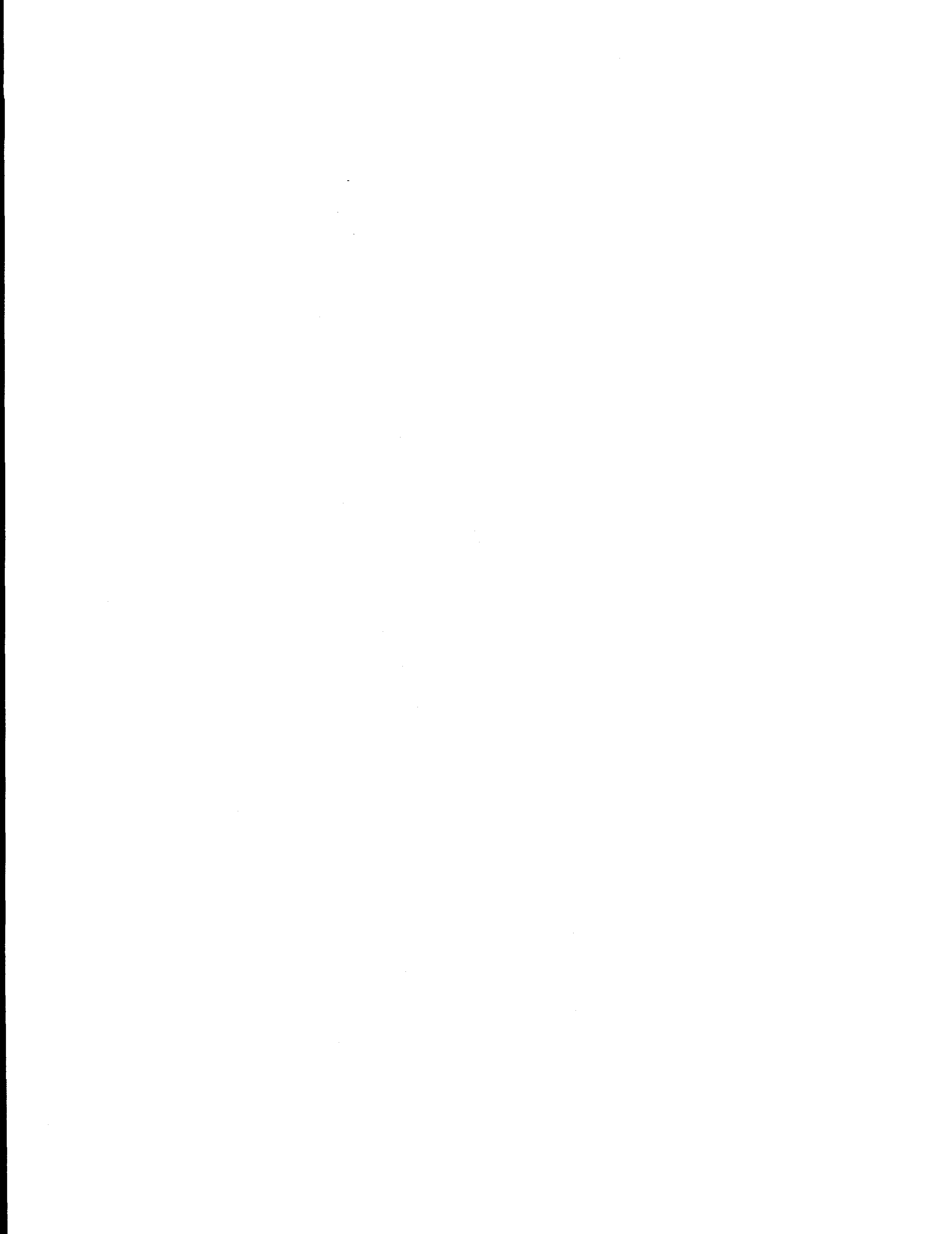

ADEPT: A GENERAL PURPOSE NUMERICAL DEVICE SIMULATOR FOR MODELING SOLAR CELLS IN ONE-, TWO, AND THREE-DIMENSIONS

Jeffery L. Gray
School of Electrical Engineering
Purdue University
West Lafayette, IN 47907-1285

ABSTRACT

This paper describes ADEPT (A Device Emulation Program and Toolbox), a numerical simulation code for modeling solar cells composed of a variety of semiconductor materials in one, two and three spatial dimensions. Material models for silicon, GaAs, AlGaAs, $CuInSe_2$, CdTe, CdS, and thin film Si:H have been implemented. One-dimensional simulations can be run easily in a personal computer environment.and recent advances in sparse matrix solvers makes it possible to run 2D simulations on small workstations.

INTRODUCTION

The photovoltaic community has demonstrated and proposed a wide variety of solar cell structures using a wide range of photovoltaic semiconductor materials. Numerical modeling has proved to be a valuable tool in understanding the operation of these devices. There are several numerical solar cell simulation programs in use. In particular, from Purdue there are TFSSP, SCAP1D, SCAP2D, PUPHS, and PUPHS2D. These have been used to model a number of solar cells - thin-film Si:H, CdS/CIS, CdS/CdTe, Si, Ge, & GaAs cells in one spatial dimension and high efficiency Si and GaAs solar cells in two-dimensions.

One-dimensional simulations are usually adequate for conventional geometry solar cells, especially at low solar intensities and for semiconductor materials that are not well characterized. At high intensities, 2D effects can become important even in conventional geometry solar cells and many high efficiency cell designs require 2D simulations or even 3D simulations. The interdigitated back contact solar cell is an example of a 2D geometry and the point contact solar cell is an example of an inherently 3D geometry.

While the basic approach to modeling any of these devices is essentially the same, special purpose codes have typically been developed for each material. This usually makes modification tedious since many different codes must be updated and tested.

ADEPT (A Device Emulation Program and Toolbox) has been developed to address this problem by unifying the common components of all these codes. In addition, ADEPT is being developed to be a tool to examine novel materials and device structures.

Numerical modeling of solar cells can be divided into six primary categories:

1) Fundamental physics
2) Material models
3) Spatial dimensionality
4) Numerical methods
5) Device analysis
6) User interface

ADEPT has been developed so that a modification in any one category has little, if any, affect on the other categories. This is a unique feature of ADEPT and accounts for its flexibility, as well as for its ability to be customized for a specific application. Each of these categories will be addressed individually below. Other papers presented in the proceedings of this conference give results of solar cell analysis using ADEPT [1-3].

ADEPT

ADEPT has been developed to be a flexible research tool for the design and analysis of solar cells. It is written in C and C++. The code is designed so that new material models can be easily and quickly incorporated. A variety of analyses are available. These include illuminated IV characteristic, dark IV, and spectral response. Other analyses can be added with minimal effort. ADEPT is also designed for maximum portability. Appropriately configured versions have been run on an IBM AT, a Mac IIci, a SUN workstation, and a super mini. Future plans include implementation on a MasPar MP1216 (16,384 parallel processors, 1.3 GFlops) and a Cray YMP2. Naturally, there are constraints associated with smaller and slower environments.

Fundamental Physics

The performance of solar cells can be modeled quite accurately by three nonlinear partial differential equations commonly known as the semiconductor equations. These equations are based on a drift-diffusion description of carrier transport.

$$\nabla \cdot D = q(p-n+N)$$

$$\nabla \cdot J_p = q(G_p - R_p \frac{\partial p}{\partial t})$$

$$\nabla \cdot J_n = -q(G_n - R_n \frac{\partial n}{\partial t})$$

CH2953-8/91/0000-0436 $1.00 © 1991 IEEE

with

$$D = -\varepsilon \nabla V$$

$$J_p = -q\mu_p p \nabla(V-V_p) - kT\mu_p \nabla p$$

$$J_n = -q\mu_n n \nabla(V+V_n) + kT\mu_n \nabla n$$

Written in this form, all the material dependent physics is relegated to relatively few terms: the generation rate terms, Gp and Gn; the recombination rate terms, R_p and R_n; the trapped charge concentration, N; the dielectric constant, $\varepsilon/\varepsilon_0$; the carrier mobilities, μ_p and μ_n; and the band parameters, V_p and V_n. The numerical solution can then be based strictly on this form and is completely independent of the specific photovoltaic materials being modeled.

Material Properties

Every material model must supply the same basic information to the solver. These are the terms ε, N, G_p, R_p, G_n, R_n, μ_p, μ_n, V_p, and V_n above. N accounts for trapped charge (donors, acceptors, and other midgap charge), G is the generation rate (optical generation, impact ionization), R is the recombination rate (radiative, Auger, SHR, tail states, etc), μ is the mobility (field dependency can be included), and V_p and V_n are the band parameters which can account for degeneracy and a nonuniform band structure. New models (for recombination or bandgap narrowing, for example) can easily be inserted.

Specific material models which have already been included are:

Silicon
GaAs
AlGaAs
CIS ($CuInSe_2$)
CdTe
CdS

A generic material model is also available for which the user defines the basic properties of the material. New models can be easily added as well.

Spatial Dimensionality

A key feature of ADEPT is its ability model devices in an arbitrary number of spatial dimensions constrained only by the computing power available. This was done by dividing each 1D, 2D, or 3D domain into elements and defining the attributes of the element in a manner independent of the number of spatial dimensions. By doing so, all material models and discretization schemes can be used independently of the dimensionality of the problem. Some benefits of this, for example, are that a single analysis routine (say, an illuminated IV) and semiconductor material model can be used for 1D, 2D, as well as 3D simulations.

Numerical Methods

ADEPT discretizes the semiconductor equations on a mesh, linearizes them, and solves for the unknowns using a generalized Newton method. Each Newton iteration requires the solution of a matrix equation whose order is three times the number of nodes in the discretization mesh. In 1D, this matrix equation can be solved quickly using a standard banded matrix solver - even on a PC. In 2D and 3D, however, the storage requirements become quite large and it is necessary to solve the large sparse matrix equations using sparse matrix techniques. We have used a sparse matrix software package, NSPCG, developed at the University of Texas-Austin. A sparse matrix method from this package, Incomplete Cholesky decomposition for matrix preconditioning and a generalized minimal residual solver (GMRES), applied to 2D simulation is more efficient than a standard direct banded matrix solver by a factor 10 in both CPU time and memory requirements. This should make 2D simulation possible on 386 and 486 IBM compatible personal computers. Two-dimensional simulations are now run routinely on a Sun4/110.

ADEPT has been written so that different matrix solvers can be used and compared. For instance, some work is being done at Purdue on applying parallel computing algorithms (using the MasPar) to the matrices arising from solar cell simulation.

Device Analysis

Simulation of specific terminal characteristics is the main objective of any device simulator. ADEPT has the capability of producing a dark IV, a typical solar cell analysis under a specified solar spectrum, and spectral response. Because of the modularity of ADEPT, new analyses can be easily and quickly incorporated. Transient and small signal steady steady state analyses are under development.

A powerful feature of numerical simulation is the ability to examine the spatial dependence of any model internal parameter, such as the recombination and generation rates, the electric field, the current densities, the carrier concentrations, etc. These examinations often lead to insights into device performance that are difficult to acheive in any other way.

User Interface

This is the component which is necessarily the most machine dependent. A portable batch processor developed in ADEPT handles both input and output. Output (internal parameters, terminal characteristics, etc.) is in a tabular form consistent with many plotting packages. Custom user interfaces for popular environments (PC, Mac, SUN) are presently being created.

SUMMARY

A *flexible numerical* simulation program for the modeling of solar cells in one-, two-, and three-dimensions has been developed. Many specific semiconductor material models have been implemented, as well as a user definable material model. Two-dimensional simulations can be run routinely on small workstations.

ACKNOWLEDGEMENT

This work was made possible, in part, by the Solar Energy Research Institute under Subcontract Number XN-0-10013-1, by Sandia National Laboratories under Document Number 12-6374, and by the Indiana Business Modernization and Technology Corporation.

REFERENCES

[1] Steven M. Durbin and Jeffery L. Gray, "Numerical Modeling of Photon Recycling in High Efficiency GaAs Solar Cells," 22nd IEEE Photovoltaic Specialists Conference, Las Vegas Nevada, October, 1991.

[2] R. J. Schwartz, J. L. Gray, and Y. J. Lee, "Design Considerations for Thin Film CIS and other Polycrystalline Heterojunction Solar Cells," 22nd IEEE Photovoltaic Specialists Confer-ence, Las Vegas Nevada, October, 1991.

[3] Youn Jung Lee and Jeffery L. Gray, "Numerical Modeling of CdS/CdTe Solar Cells: A Parameter Study," 22nd IEEE Photovoltaic Specialists Confer-ence, Las Vegas Nevada, October, 1991.

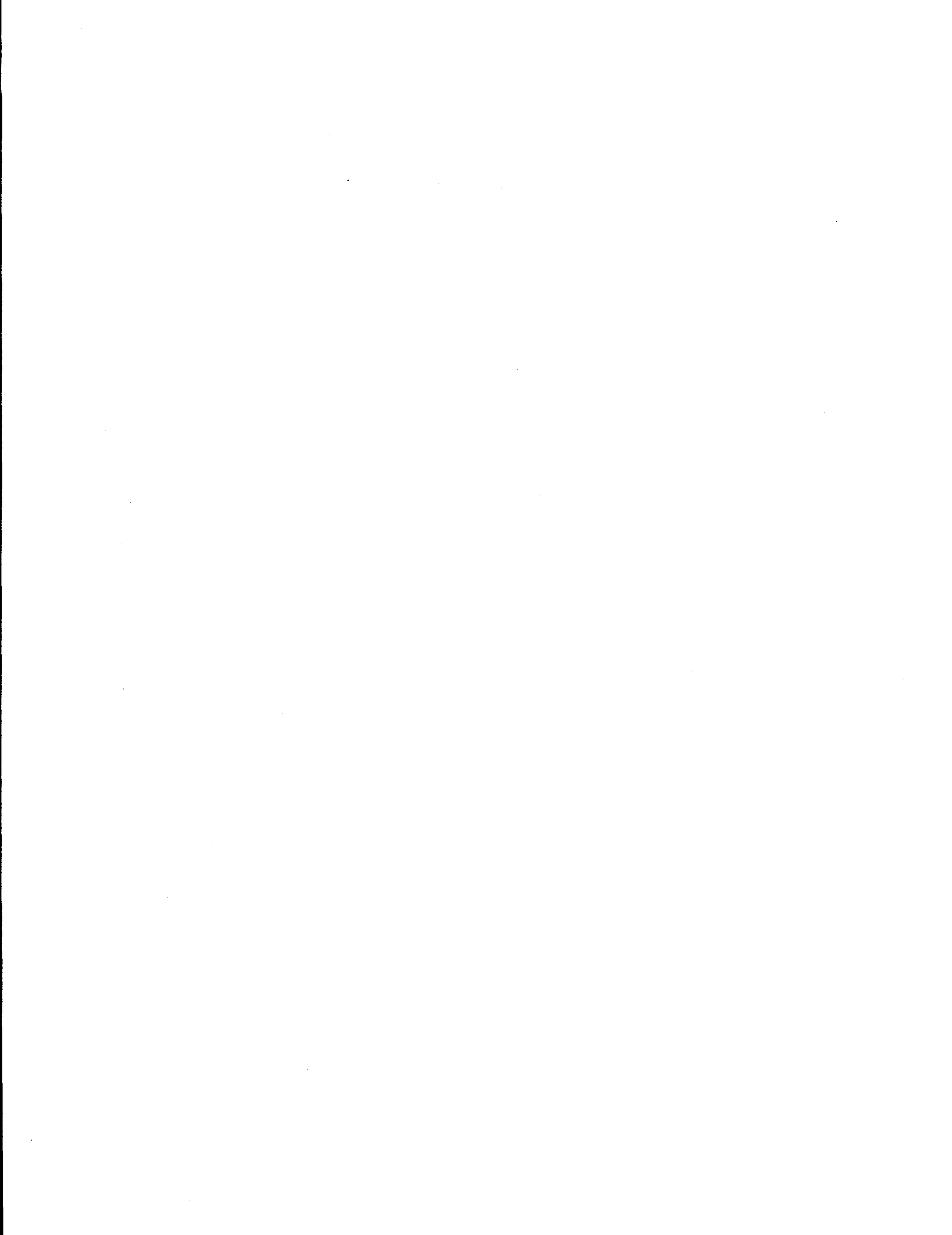

Appendix B

This appendix contains a copy of a paper entitled "Numerical Modeling of CdS/CdTe Solar Cells: A Parameter Study" that was presented at and appears in the Conference Record of the Twenty-Second IEEE Photovoltaic Specialists Conference in Las Vegas, Nevada, October 1991.

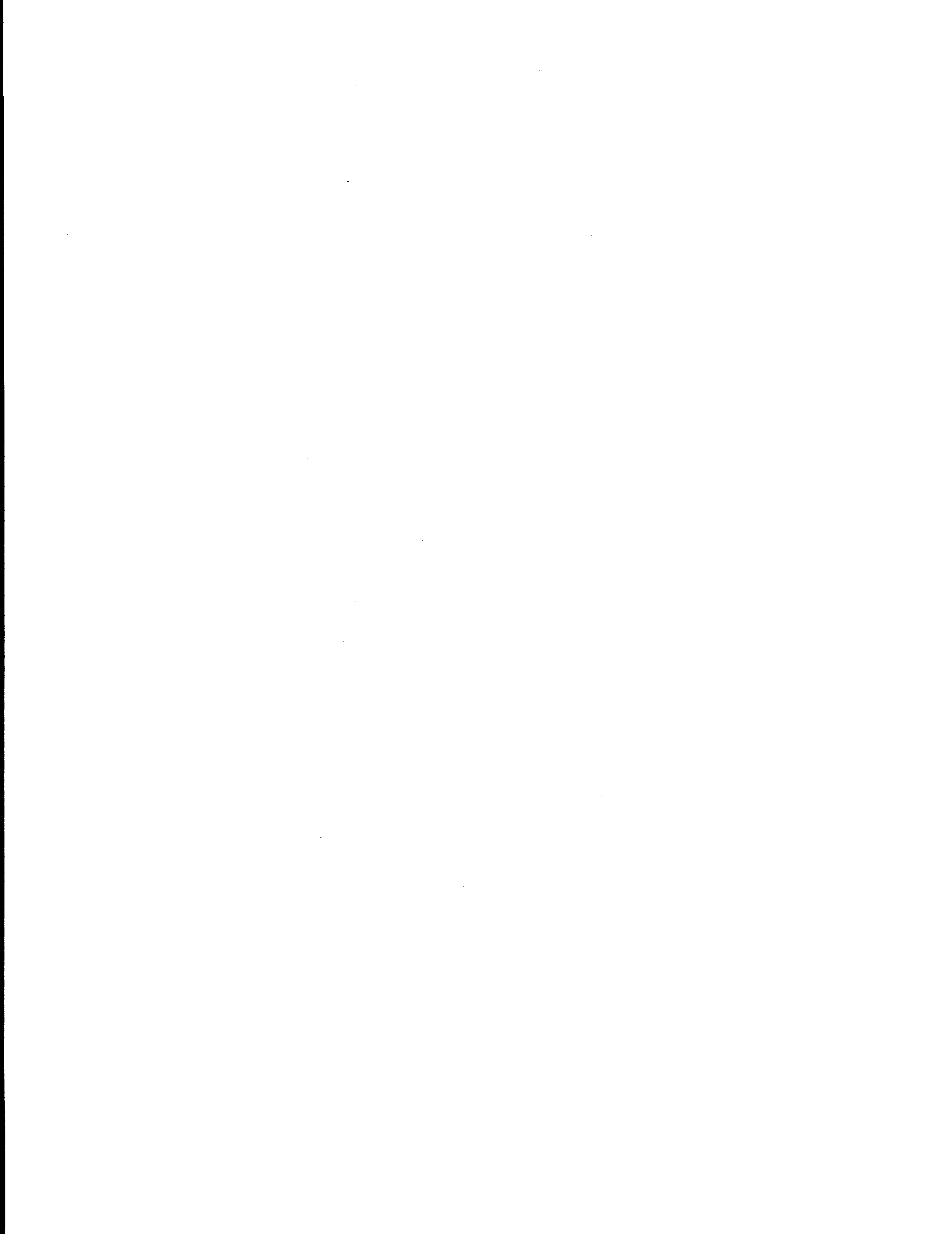

NUMERICAL MODELING OF CdS/CdTe SOLAR CELLS: A PARAMETER STUDY

Youn Jung Lee and Jeffery L. Gray

School of Electrical Engineering
Purdue University
West Lafayette, IN 47907

ABSTRACT

CdTe based solar cells are candidates for inexpensive and relatively efficient solar cells. Efficiencies of as high as 13.4% have been reported for these cells. In order to evaluate the potential of these cells, numerical modeling is performed to analyze the factors that limit cell performance. The purpose of this paper is to model the effects of the pertinent material parameters on predicted cell performance so that a better understanding of the material characteristics can be achieved. Numerical modeling is performed to determine a set of material parameters consistent with measured cell performance. These parameters can then be used to make realistic performance projections.

INTRODUCTION

CdTe is a promising material for solar cells. In order to produce an inexpensive and very efficient CdTe based solar cells, it is necessary to understand the processes which limit performance. This can be carried out by numerically modeling the CdTe solar cells and comparing the output with measured solar cell performances. The basic material parameter values were gathered from a numerous published literatures and the dependence of solar cell performance on these parameters is sought.

In this paper, a 1D numerical solar cell simulation program is used to analyze the operation of these devices. Since CdTe is not a well characterized material, the purpose of this paper is to model the effects of the pertinent material parameters on predicted cell performance so that a better understanding of the material characteristics can be achieved.

APPROACH

An extensive review of the literature has been performed to tabulate both measured cell performance and material parameters. Table 1 lists the measured performance characteristics of CdTe based solar cells as reported in the literature. Table 2 lists CdTe material parameters as reported in the literature.

A general purpose numerical solar cell simulation program developed at Purdue was used to perform this parameter study. ADEPT (A Device Emulation Program and Toolbox) solves the three coupled nonlinear semiconductor equations on a discrete grid. From this solution, the terminal characteristics of the solar cell can be computed. In addition, internal parameters such as spatial recombination rate, can be examined in detail.

Since there is a wide range of values reported for many of the material characteristic parameters, sometimes contradictory, it was necessary to model the effect of a number of parameters on cell performance and compare the predicted performances with the measured results. In the paper we examine the effects of intrinsic carrier concentration, conduction band offset, interface recombination velocity, and carrier mobility on predicted cell performance. The ultimate goal is to determine a unique set of material parameters for CdTe which accurately predict cell performance.

DISCUSSION

The basic structure of CdS/CdTe solar cell used for this parameter study was taken from reference [3].

Intrinsic Carrier Concentration

The simulation carried out using the cited values of effective density of states predicted unrealistically high open circuit voltage. These values of effective density of states also lead to a significantly smaller value of n_i than that listed in Table 2.

In order to bring the simulated cell performance near the experimental results, the effective density of states of conduction band had to be raised. It was found that Nc should be at least 9.0e18 cm^{-3}. In fact, this agrees well with the value of Nc determined from the ratio of effective masses. i.e.,

$$\frac{N_C}{N_V} = \frac{N_C}{1.27e19} = \left(\frac{m_n^*}{m_p^*}\right)^{3/2}$$

The value of N_C from above equation was 9.96e18 cm^{-3}. The effect of N_C, and hence n_i, on the open circuit voltage is shown in Figure 1.

CH2953-8/91/0000-1151 $1.00 © 1991 IEEE

Conduction Band Offset

The electron affinity, χ, of CdTe is generally taken to be slightly smaller than that of CdS (4.3eV), its exact value can have an influence on predicted cell performance. A number of simulations were performed changing only the electron affinity of the CdTe. The results show that the open circuit voltage decreased slightly with increasing electron affinity of CdTe until the conduction bands of the two layers line up, then there is no change as the CdTe electron affinity increases further, since the Fermi energy pins at the conduction band edge. The band offset controls the spatial extent of the depletion region. For $\chi_{CdTe} < \chi_{CdS}$, the depletion width into the CdTe is smaller than when $\chi_{CdTe} > \chi_{CdS}$. This can be seen in Figures 2 and 3. Recombination in the depletion region has a strong influence on the open circuit voltage. Figure 4 shows the recombination rate in the CdTe for the two cases depicted in Figures 2 and 3 at open circuit. Note the high level of recombination, and hence a lower open circuit voltage for the $\chi_{CdTe} > \chi_{CdS}$ case.

Interface Recombination Velocity

Although it is typically thought that recombination at the window layer/CdTe will have a major influence on cell performance, the simulations do not substantiate this assumption. When CdS/CdTe solar cell was modeled with S=0 and S=2.0e6 cm/s at the interface, almost no difference in performance is predicted. This is due to the fact that band bending at the heteroface junction shifts the collecting junction (i.e. the point at which the material changes from p-majority carrier to n-majority carrier) away from the interface into the CdTe. This can be easily seen from the energy band diagram of Figure 5. Since most of the excess carriers are created in the CdTe, they need only to reach the collecting junction before they recombine. Thus, the heteroface is effectively screened out and cell performance is nearly unaffected.

Carrier Mobility and the Back Contact

Figure 6 shows the effect of CdTe minority carrier mobility and back surface effective recombination velocity on the short circuit current. The back surface has little effect on the short circuit current except for the highest simulated mobilities. This is because most of the carriers are created with the CdTe depletion region and are collected by the drift field. This also decreases the sensitivity of the cell to the mobility value. The short circuit current varies by only about 10% for mobilities ranging from 10 to 650 $cm^2/V\text{-}s$.

SUMMARY

A parameter study of some of the CdTe material parameters has been performed. A range of values for these parameters has been determined which gives realistic performance predictions. More work is needed to fully understand the roles of these parameters on cell performance and to construct an accurate model which can be used to make performance predictions.

ACKNOWLEDGEMENT

This work was supported by the Solar Energy Research Institute under Subcontract Number XN-0-10013-1.

Table 1 Survey of Measured CdTe Cells

window	Voc [V]	Jsc [mA/cm^2]	FF	Effi.	Ref.
CdS	0.725	21.23	0.67	10.31	[7]
	0.7484	22.21	0.6339	10.5	[15]
	0.75	22.7	0.62	10.5	[52]
	0.754	27.9	0.61	12.8	[29]
	0.748	22.2	0.634	10.6	[14]
	0.612	20.5	0.605	8.7	[10]
	0.67	20		11.7	[54][55]
	0.74	22		10.4	[30]
	0.78	22.5	0.58	11.6	[34]
	0.797	21.1	0.672	11.3	[50]
	~0.5	~20	~0.5	~5	[42]
	0.82	21		8	[8]
	0.759	18.6	0.57	8.8	[39]
	0.783	24.98	0.627	12.3	[3]
	0.747	21.69	0.657	10.6	[17]
	0.747	17.3	0.67	8.7	[25]
	0.72	27.9	0.65	13.1	[32]
	0.68	20.5	0.56	7.9	[36]
	0.84	21.9	0.725	13.4	[47]
	0.79	26.2	0.615	12.7	[47]
	0.81	19.5	0.73	11.5	[47]
	0.715	24.2	0.60	10.3	[47]
	0.765	20.9	0.715	11.0	[47]
	0.797	21.1	0.672	11.3	[49]
ITO	0.81	20	0.55	10.5	[53]
	0.72	19	0.6	8.2	[13]
	0.84	6.5		3	[12]
	0.89	20		13.4	[37]
TO	0.663	28.1	0.563	10.5	[32]
CdTe	0.83	19.7	0.67	10.5	[18]
	0.82	21		10.7	[6]
	0.723	12	0.63	6	[31]
ZnO	0.45	18	0.41	4.8	[20]
thin film single crys.	0.48 ~ 0.53 0.54	 12.5 19.5		 3.7 7.6	[51]
	0.54	19.5		8.8	[5]
Au	0.807	20.9	0.67	15.1	[50]
$Zn_{0.3}Cd_{0.7}S$	0.78	23.4	0.594	10.84	[16]

Table 2 CdTe Material Parameters

	Values	References
Eg [eV]	1.51 (n - type) 1.46 (p - type)	[38]
	1.5	[10][9][15][26][42]
	1.45	[21][35][45][44][41]
	1.44	[22][40][24]
	1.46	[28]
μ [$cm^2 V^{-1} s^{-1}$]	60 - 250 (n -type)	[48]
	5 - 10 (n- type)	[11]
	40 - 45 (p - type)	[10]
	65	[9]
	1200 at 170 K	[27]
	159 (p - type)	[28]
	800	[24]
	μp=60 μn=600	[43]
	40 - 60 (Hall)	[1]
	50 (Hall)	[2]
	4 (at the junction)	[46]
	μp=5 μn=50	[23]
	μn = 4	[25]
ao [nm]	0.648+-0.002	[24]
mn*	(0.11+-0.01)mo	[27]
	0.1 mo	[46]
mh*	0.12 mo	[19]
	0.4 mo	[46]
ni [/cm^3]	1.0e7	[40]
Nc [/cm^3]	8.65e17	[24]
	7.94e17	[23]
Nv [/cm^3]	1.27e19	[23]
dielectric constant	7.21	[22]
	10.31 (static) 7.6 (optical)	[27]
	9.6	[23][24]
electron affinity [eV]	4.28	[40][16]
t [nsec]	6.7 for calculations, tn = 160, tp = 0.8	[9]
	100	[1]
	0.06	[33]
SI [cm/sec]	2.0e6	[33][23]

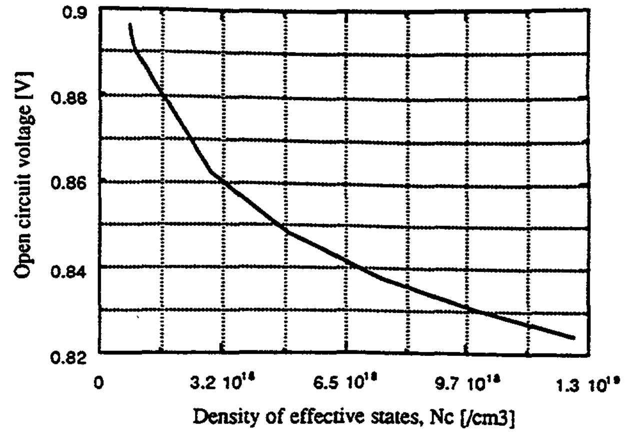

Figure 1. The open circuit voltage dependence on the conduction band effective density of states.

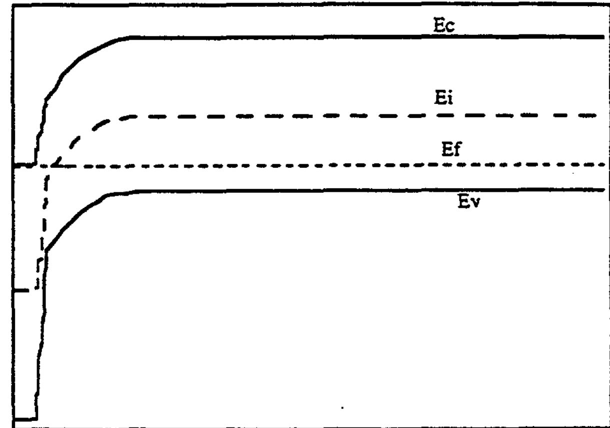

Figure 2. Energy band diagram for $\chi_{CdTe} = 3.9$ eV.

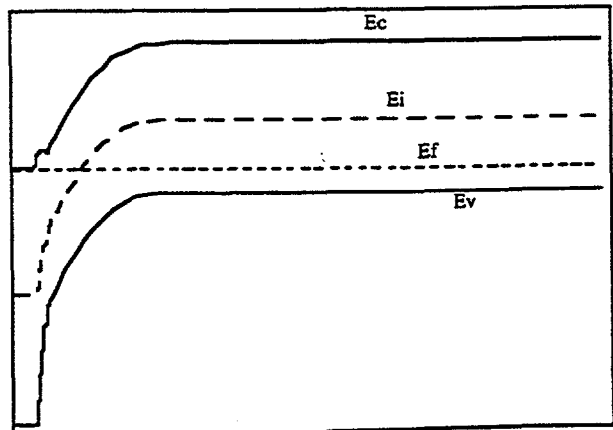

Figure 3. Energy band diagram for $\chi_{CdTe} = 4.7$ eV.

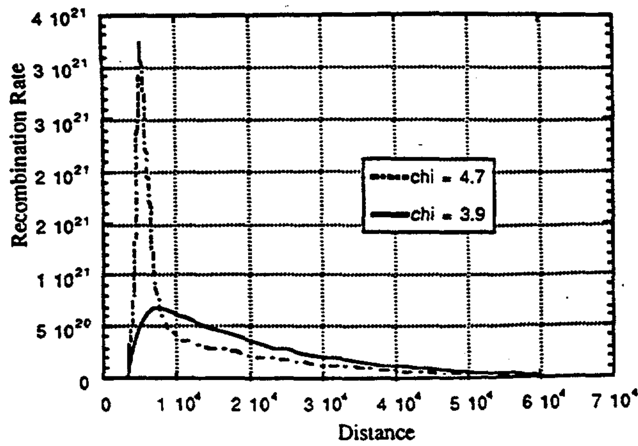

Figure 4. Recombination rates for the two cases shown in Figures 2 and 3.

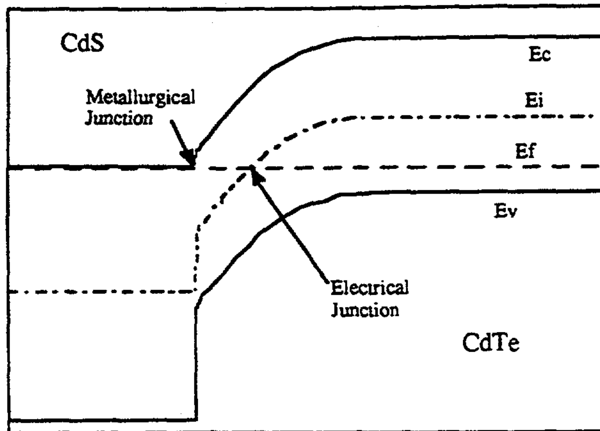

Figure 5. Energy band diagram showing the relative positions of the metallurgical and electrical junctions.

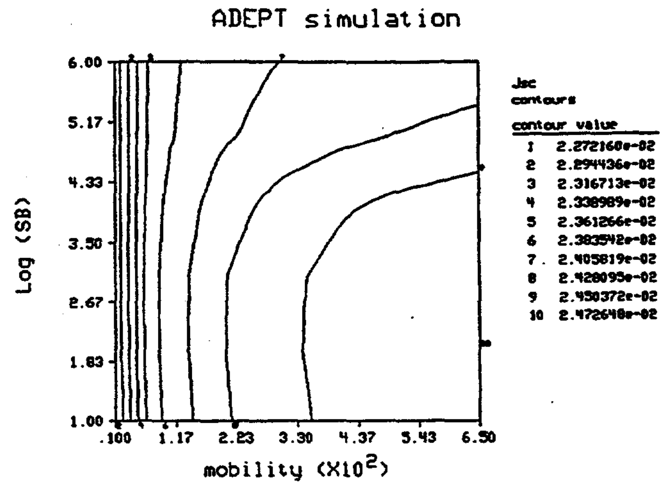

Figure 6. Short circuit current as a function of both minority carrier mobility and the logarithm of the back surface recombination velocity

Appendix C

This appendix contains a copy of a paper entitled "Design Considerations for Thin Film CIS and Other Polycrystalline Heterojunction Solar Cells" that was presented at and appears in the Conference Record of the Twenty-Second IEEE Photovoltaic Specialists Conference in Las Vegas, Nevada, October 1991.

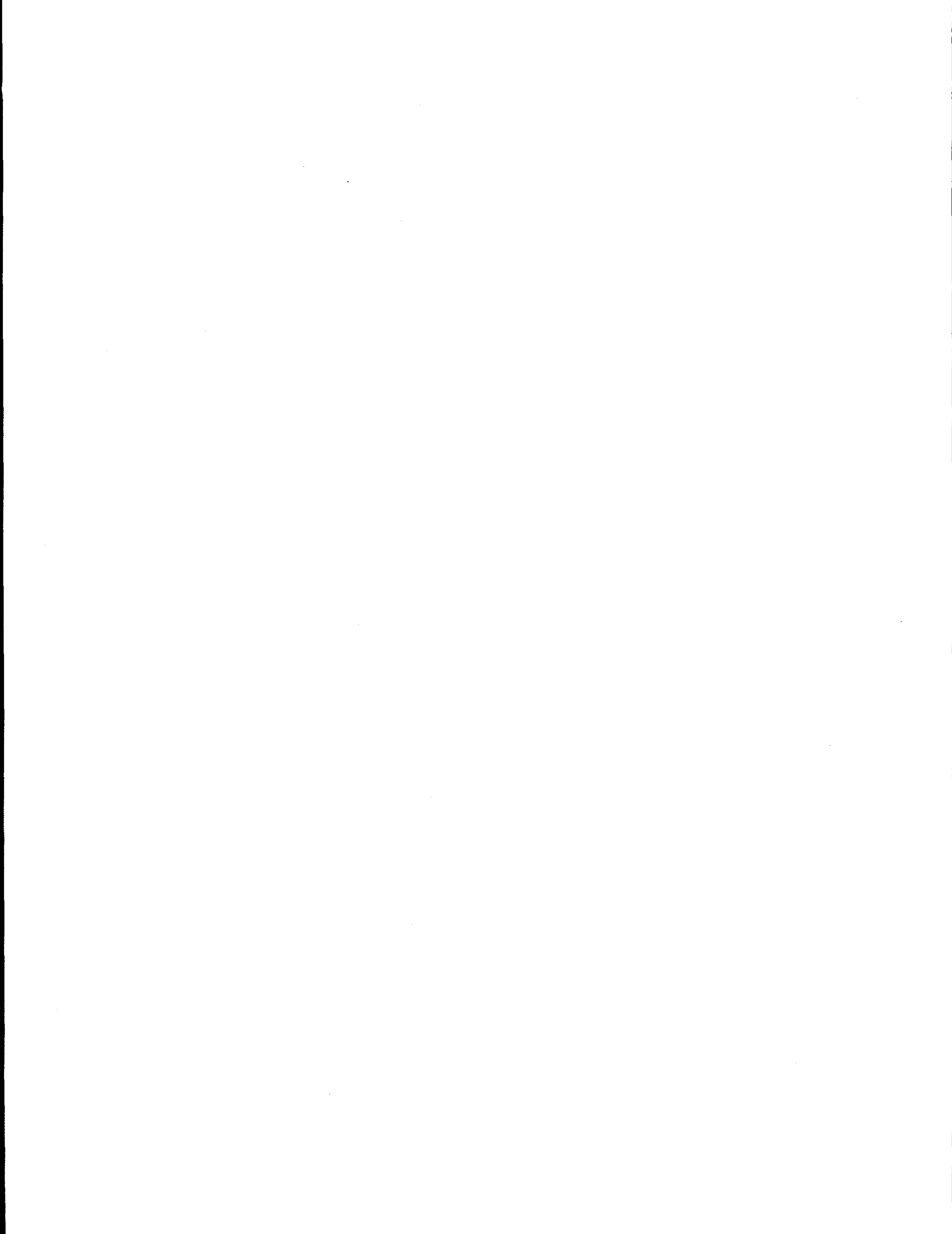

Design Considerations for Thin Film $CuInSe_2$ and other Polycrystalline Heterojunction Solar Cells

R. J. Schwartz, J. L. Gray and Y. J. Lee
School of Electrical Engineering
Purdue University
West Lafayette, IN 47907

Abstract

Many thin film heterojunction solar cells contain an interface between the emitter and base which is a very high recombination region and which effectively prevents the passage of minority carriers. However, by utilizing proper design techniques which will be discussed here, the problem can be minimized; efficient thin film heterojunction solar cells can be fabricated, even though they contain high recombination interfaces between the emitter and base regions. Numerical calculations of the performance of $CdS/CuInSe_2$ cells are used to illustrate the effects of the design considerations presented.

Introduction

Thin film heterojunction solar cells fabricated by high throughput techniques such as evaporation, sputtering or chemical vapor deposition have an interface region between the dissimilar materials which can be expected to have very high recombination associated with it. In fact, except in those cases where epitaxial growth of lattice matched materials occurs, this interface region might reasonably be expected to pass few minority carriers. One possible example of such an interface is the region between the CdS emitter and the $CuInSe_2$ base of a CIS solar cell. And yet, it is well known that some of the most efficient thin film solar cells have been fabricated using methods which presumably produce this high recombination layer.

The purpose of this presentation is to discuss design considerations which allow the fabrication of efficient thin film solar cells in spite of the presence of such "dead" layers. CIS thin film cells are used as a particular example but the conclusions apply to a variety of thin film cells. The vehicle used to illustrate the effects of the application of these design principles will be the the results of numerical simulations of $CdS/CuInSe_2$ solar cells, since these cells are reasonably mature in both their modeling and fabrication and offer experimental verification of the theory presented.

Materials Choice

Emitter and base materials used in heterojunction solar cells are frequently chosen for their band gaps and the compatibility of their processing and deposition. In this paper we shall see that the performance of thin film heterojunction solar cells may depend on more than the usual parameters of band gap, mobility, and lifetime. The electron affinity differences between the base and emitter materials as well as the electron affinity of the transparent conducting emitter contact material, can be crucial to efficient cell operation. We will show the strong dependence of efficiency upon the electron affinities of the various materials used in the fabrication of the cells.

The three design rules discussed below are applicable when the interface region between the emitter and base results in the recombination of minority carriers which attempt to traverse this region.

Design Rule 1

Choose the emitter and base materials and doping so that the base region nearest the emitter is inverted.

Fig. 1 shows the equilibrium band diagram for a series of $CdS/CuInSe_2$ solar cells with emitters doped to $N_d = 1 \times 10^{18}$ cm^{-3} and bases doped to $N_a = 1 \times 10^{16}$ cm^{-3} and a range of electron affinity differences be-

CH2953-8/91/0000-0920 $1.00 © 1991 IEEE

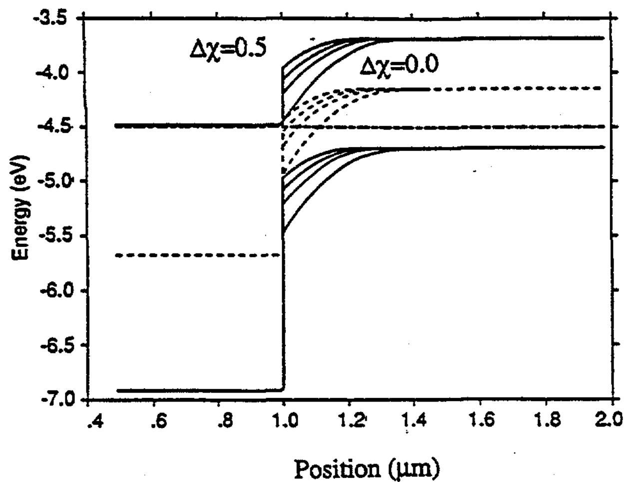

Fig. 1 Equilibrium band diagram for electron affinity differences of 0, .25, .4 and .5 ev.

tween the emitter and base materials ($\Delta\chi$ = 0.0, 0.25, 0.4, and 0.5 ev). It is important to note that strong band bending in the base, near the emitter-base interface, occurs when the electron affinity of the emitter is equal to that of the base i.e., the electron affinity difference, $\Delta\chi$, is 0.0 ev. In fact, under this condition the base is strongly inverted in this region. As the electron affinity of the emitter grows larger than that of the base, the strength of the electric field in the inversion region falls and the width of the inversion region shrinks; eventually, the inversion region disappears when $\Delta\chi \approx 0.5$ ev. .This observation of the existence of an inversion region is crucial to the design of efficient thin film solar cells which may contain high recombination layers at the emitter-base interface.

The reason for the importance of this inversion region is seen in Fig. 2, where we have compared the performance of two solar cells. One has a strongly inverted layer ($\Delta\chi$ = 0.0 ev) and the other has a weakly inverted layer $\Delta\chi$ =0.4 ev). In the simulation presented here, both of these cells contain a layer between the emitter and the base which is a very high recombination region. The recombination is so high, in fact, that minority carriers have a difficult time passing through the region without recombining. This is the situation which one would expect to encounter when the emitter and base are composed of dissimilar materials with

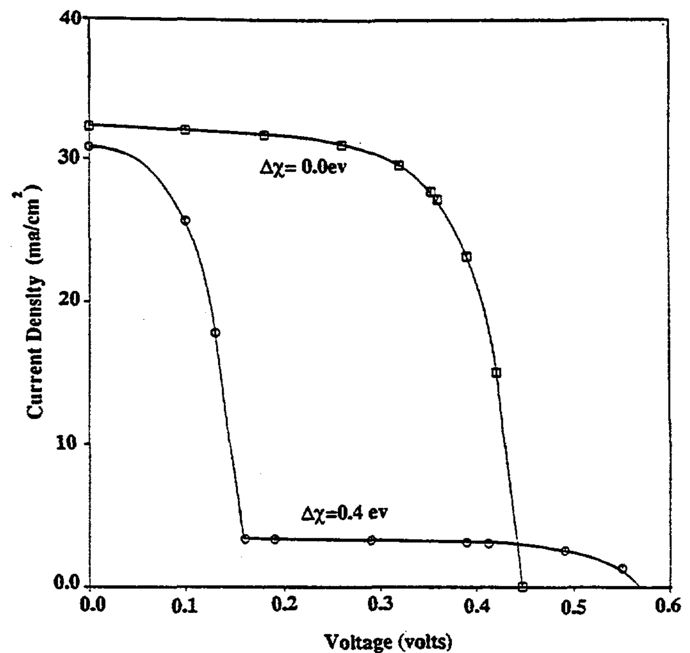

Fig. 2 I-V characteristics for cells with electron affinity differences of 0.0 and 0.4 ev.

different lattice constants or when the cell growth process is interrupted between the growth of the emitter and base.

Note that the cell which is strongly inverted shows a classic I-V curve; the weakly inverted cell exhibits a rapid drop in current for small positive voltages. Both cells must pass their total current through a high recombination region. The strongly-inverted-base cell does this successfully; the weakly-inverted-base cell does not. The reason the strongly-inverted-base cell successfully collects the current is that a minority carrier is "collected" when it moves to a region in which it is a majority carrier. Thus, in the case of the inverted base cell, electrons which are generated in the base beyond the inversion region and which move toward the emitter to be collected do not have to move all the way to the emitter to be collected. They become "collected" when they reach the inversion region and hence do not have to traverse the high recombination layer as minority carriers. On the other hand, minority carriers generated in the emitter must traverse the high recombination region in order to reach the p-type base region and become collected. Thus, even the strongly-inverted-base cell of Fig. 2 suffers a loss of the holes which are generated in the emitter.

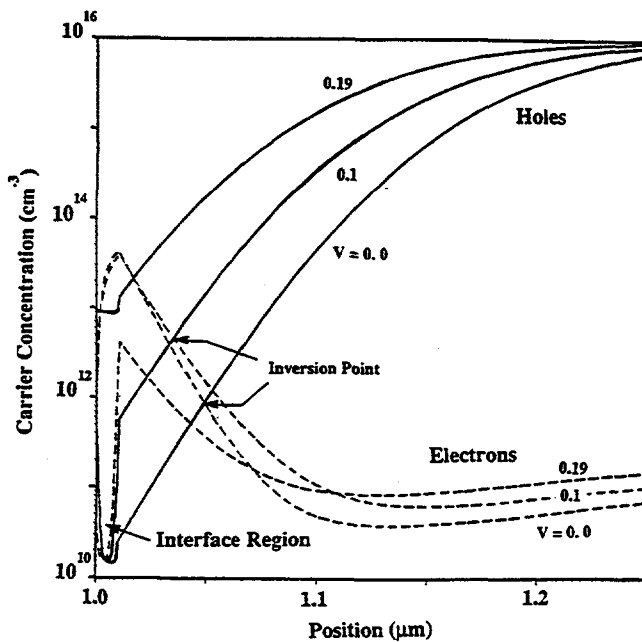

Fig. 3 Hole and electron concentrations in the base, in the vicinity of the emitter-base interface, for a cell with $\Delta\chi$ = 0.4 ev.. Cell voltages are 0.0, 0.1 and 0.19 v.

Fig. 3 shows the hole and electron concentrations in the base near the emitter-base interface of the weakly-inverted-base cell for biases of 0.0, 0.1, and 0.19 volts. The weakly-inverted-base cell does a reasonable job of collecting electrons generated in the base when operating at 0.0 volts. At 0.0 volts the inversion region exists and electrons generated in the base are collected without having to traverse the high recombination interface. However, as the the cell becomes forward biased, the inversion region rapidly becomes thinner (Fig. 3, V = 0.1). Once the forward bias is sufficiently large that the inversion region disappears (Fig. 3, V = 0.19) all minority carriers must traverse the high recombination interface region in order to be collected. This rapid loss of the inversion region results in the dramatic change in the I-V curve, shown in Fig. 2, for a cell with an electron affinity difference between the emitter and base of 0.4 ev..

From this example we see that not only must there be an inversion region but it must be sustainable over the full operating of the cell.

DESIGN RULE 2

Minimize the thickness of the emitter.

The computed spectral response for cells with and without a high recombination layer and with thick and thin emitters are shown in Fig. 4. Note that for all of these cells any holes which are generated in the emitter must traverse the interface region before they become collected. For the cells with a high recombination layer between the emitter and base, nearly all of the carriers generated in the emitter will recombine before they are collected by the base independent of the existence of an inversion layer in the base.

The cell with a relatively thick emitter (1.0 µm) exhibits poor spectral response in the blue end of the spectrum; many of these photons create holes in the emitter which then recombine as they attempt to pass through the high recombination interface.

If the emitter is sufficiently thin, relatively few holes are generated in the emitter and more of the high energy photons penetrate to the base where the carriers which are generated can be collected. In Fig. 4, we see that reducing the emitter thickness from 1.0 µm to 0.2 µm in the presence of a high recombination interface

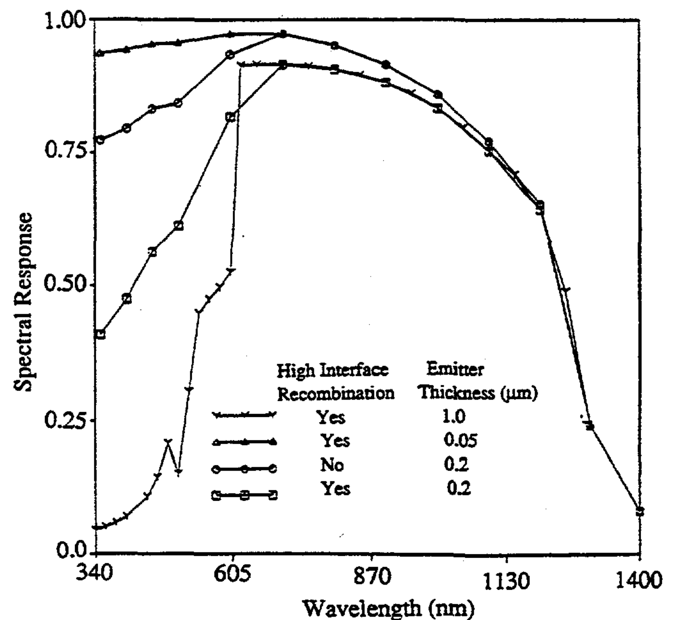

Fig. 4 Spectral response for cells with and without a high recombination interface and for emitter thicknesses of 0.05, 0.2 and 1.0 um. $\Delta\chi = 0.0$ ev.

improves the blue response (as expected). Removing the high recombination interface increases the blue response of a cell with a 0.2 μm even further. A further reduction in the thickness of the emitter to 0.05 μm results in excellent blue response even in the presence of the high recombination interface.

It is no accident that the highest reported short circuit currents and highest efficiencies occur in CIS cells which have emitters as thin as 3 to 5 nm.

Design Rule 3

Choose a transparent contact material with high optical transmission and low electron affinity.

For very thin emitters, the space charge region may extend entirely through the emitter. Under these circumstances, the field in the space charge region will be strongly influenced by the electron affinity of the transparent contact. The actual field in the emitter will depend on the electron affinity and the location of the Fermi level in the contact material. It will become nearly independent of the doping in the emitter. In this case, the existence and strength of the inversion layer in the base will be dominated by the electron affinity differences of the contact and the base and location of the Fermi level in the contact material.

For very thin emitter cells, one would like to choose contact materials which are transparent over a broad spectral range, have high conductivity and low electron affinity.

Summary

The design considerations presented herein rationalize some of the solar cell designs already in use and may be applicable to a wide variety of heterojunction thin film solar cells.

Acknowledgments

This work was supported by the Solar Energy Research Institute.

Appendix D

This appendix contains the user's guide to ADEPT/F (1D Fortran version) for IBM compatibles.

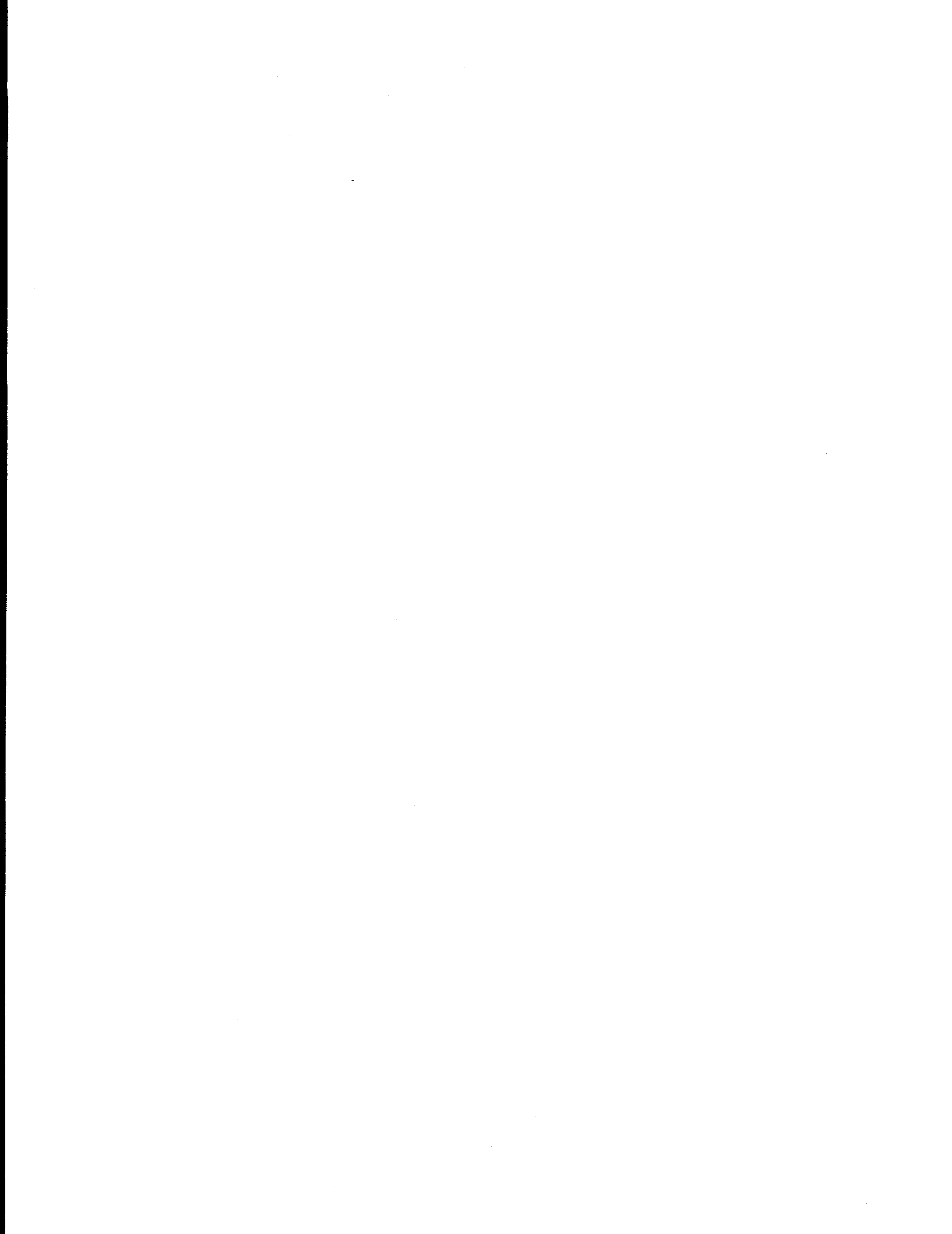

ADEPT/F FOR IBM PC REFERENCE GUIDE

Release Information

This release is being provided at no charge. Future releases will contain more features and more complete documentation. A small fee will be charged for future releases. Please direct comments and requests for more information to:

Jeffery L. Gray
Associate Professor
School of Electrical Engineering
1285 Electrical Engineering Building
Purdue University
West Layafette, IN 47907-1285

Phone: (317)494-3478
Fax: (317)494-6440
E-mail: grayj@ecn.purdue.edu

Installation

ADEPT/F will run on any IBM compatible with a numeric coprocessor, sufficient memory (512K is recommended) and a hard disk. However, for speed of execution, a 386 or 486 machine is desirable. See the READ.ME file on the distribution disk for installation instructions. Be sure to place the following directory in your PATH environment variable which is usually set in your AUTOEXEC.BAT file:

C:\ADEPTF\BIN

Running ADEPT/F

ADEPT/F (A Device Emulation Program & Tool/Fortran) can be invoked by using the following command line:

ADEPTF *infile* [*SPATH*]

The input deck is in *infile*. A summary of the program execution is placed in the file *infile*.sum. *SPATH* is an optional parameter which tells the program where to look for spectrum files. ADEPT/F first looks in the current directory, and, if the spectrum file is not found, will then look in the directory specified by *SPATH*. (The square brackets indicate that *SPATH* is optional. Do not include them in the specification.) If not specified, *SPATH* defaults to "C:\ADEPTF\SPECTRUM\". If you use this parameter, do not embed any blanks and do not include the double quotes.

As mentioned above, a summary of the program execution is placed in a file called *infile*.sum. In addition, ADEPT/F creates a file called *infile*.dat which contains information about the internal variables (carrier concentrations, electric fields, recombination, etc.)

The input file contains a series of 'cards' which may be of the following forms:

```
*titlecard anything at all
```

or

```
cardname var1=value1 var2=string2
+ array1=va1/va2/va3
```

The card name and continuation mark (+) must start in column 1. A 'card' can be up to 10 lines long. Any line starting with a blank or a $ is ignored. In the second example, assignment expressions cannot contain any embedded spaces. Assignment expressions must be be separated by a space, as shown above, or a comma. A sample input file and summary file are on the distribution disk.

The following tables describe the options and parameters which can be specified by the input file. Although the parameters are shown as uppercase, ADEPT/F treats uppercase and lowercase letters the same.

*TITLE

All characters following *TITLE (up to column 80) become part of a comment used to annotate the output.

SOLVE

Parameter	Type	Default	Description
ITMAX	integer	100	maximum # of Newton iterations
DELMAX	real	1×10^{-6}	convergence test (kT)
MAXDEL	real	1×10^{50}	
NDVRGE	integer	5	# of iterations for which ΔV can increase before divergence is assumed
NBACKUP	integer	3	
NDVBIG	integer	2	
METHOD	integer	1	
TAU	real	1.0	for METHOD=2

OUTPUT

Parameter	Type	Default	Description
INFO	integer	3	level of output 0 for mimimum 6 for debugging
STEP	integer	5	for tables, print values every STEP nodes
COPIES	integer	2	# copies of summary info

MESH

Parameter	Type	Default	Description
NX	integer	250	total # of nodes in F-D mesh
XRES	real	0.5	min. spatial resolution (angstroms)
MFLAG	integer	0	if =0, initial mesh is redefined based on refinement criteria described below if =1, mesh is not redefined
WT	real( )	 1.0 1.0 0.5 0.5	weighting parameters for mesh refinement WT(1), ρ slowly varying WT(2), E slowly varying WT(3), tendency for uniform mesh WT(4), tendency fo same # nodes in each LAYER
ISMTH0	integer	0	# of nodes set aside (per LAYER) for smoothing of redefined mesh
ISMTH1	integer	6	# of nodes set aside (per LAYER) for smoothing of initial mesh
XFIX	real( )	-1.	position(s) at which a node must be placed (angstroms) to enable, set XFIX(1)=0.0
NNX	integer( )	-1	# nodes to be placed between fixed node positions (positioning of these nodes is still based on redefinement scheme)

MISC

Parameter	Type	Default	Description
TEMPC	real	27.0	temperature (degreeC)
TEMPK	real	300.15	temperature (Kelvin)
VTH(300)	real	1×10^7	thermal velocity at 300 K (cm/s)

BC

Parameter	Type	Default	Description
MBC	integer	1	sets contact boundary conditions =1 for charge neutral contacts =2, then electrostatic potential at contacts set by metal work functions and semiconductor electron affinity
WDFRT	real	0.86	$\phi_M - \chi_S$ at front contact (eV)
WDBCK	real	0.86	$\phi_M - \chi_S$ at back contact (eV)
SPF	real	-1.0	surface recombination velocity for holes at x=0 (cm/s) (=−1 sets SPF=∞)
SNF	real	-1.0	surface recombination velocity for electrons at x=0 (cm/s)
SPB	real	-1.0	surface recombination velocity for holes at $x=x_{max}$ (cm/s)
SNB	real	-1.0	surface recombination velocity for electrons at $x=x_{max}$ (cm/s)

AR

Parameter	Type	Default	Description
T	real	0.0	thickness of AR layer (angstroms)
TM	real	0.0	thickness of AR layer (microns)
NDX	real	1.0	index of refraction of AR layer

GLOBAL

This card must appear before any LAYER card. The default value for each variable on the LAYER card can be changed on this card (except T, the layer thickness).

*LAYER

All characters following *LAYER (up to column 80) become part of a comment used to annotate the output. It is intended to provide additional descriptive information about the associated LAYER.

LAYER

Parameter	Type	Default	Description
T	real		thickness of layer (angstroms)
TM	real		thickness of layer (microns)
EG EGL EGR	real	1.0	bandgap (eV)
CHI CHIL CHIR	real	4.0	electron affinity (eV)
KS	real	1.0	dielectric constant
NDX	real	1.0	index of refraction
NV	real	1×10^{20}	valence band effective density of states (cm^{-3})
NC	real	1×10^{20}	conduction band effective density of states (cm^{-3})
UP	real	1.0	hole mobility ($cm^2/V{-}s$)
UN	real	1.0	electron mobility ($cm^2/V{-}s$)

LAYER (continued)

Parameter	Type	Default	Description
PROF.NA	char	LINEAR	doping profile type (only option at present)
NA NAL NAR	real real real	0.0	acceptor dopant density (cm^{-3})
NA.SIG	real	0.0	standard deviation (in eV) of gaussian distribution of acceptors
GA	real	1.0	acceptor degeneracy factor
EAA EAAL EAAR	real	0.0	acceptor energy level (eV above E_V)
XNA	real	0.0	(see notes) (angstroms)
PROF.ND	char	LINEAR	doping profile type (only option at present)
ND NDL NDR	real real real	0.0	donor dopant density (cm^{-3})
ND.SIG	real	0.0	standard deviation (in eV) of gaussian distribution of donors
GD	real	1.0	donor degeneracy factor
EAD EADL EADR	real	0.0	donor energy level (eV below E_C)
XND	real	0.0	(see notes) (angstroms)

LAYER (continued)

Parameter	Type	Default	Description
KTA.T	real	.001	characteristic energy of conduction band tail (eV)
KTD.T	real	.001	characteristic energy of valence band tail (eV)
GAMAX.T	real	0.0	density of states of conduction band tail at E_C $(cm^{-3}-eV^{-1})$ (-1. sets GAMAX.T = NC/(1eV)) (states assumed to be acceptor-like)
GDMAX.T	real	0.0	density of states of valence band tail at E_V $(cm^{-3}-eV^{-1})$ (-1. sets GDMAX.T = NV/(1eV)) (states assumed to be donor-like)
EACORN.T	real	0.0	energy below E_C at which conduction band tail begins (eV)
EDCORN.T	real	0.0	energy above E_V at which valence band tail begins (eV)
CAP.T	real	1×10^{-14}	capture cross-section for holes in the conduction band tail (cm^2)
CAN.T	real	1×10^{-14}	capture cross-section for electrons in the conduction band tail (cm^2)
CDP.T	real	1×10^{-14}	capture cross-section for holes in the valence band tail (cm^2)
CDN.T	real	1×10^{-14}	capture cross-section for electrons in the valence band tail (cm^2)

LAYER (continued)

Parameter	Type	Default	Description
A0	real	0	Radiative Recombination Coeff. (cm^3/s)
AP	real	0	hole Auger Coeff. (cm^6/s)
AN	real	0	electron Auger Coeff. (cm^6/s)
TAUP.SHR	real(5)	1×10^6	SHR hole lifetime (s)
TAUN.SHR	real(5)	1×10^6	SHR electron lifetime (s)
ET.SHR	real(5)	0.0	SHR trap level wrt E_i (eV)
NTT.SHR	real(5)	0.0	density of SHR recombination centers (cm^{-3}) (donor-like, if NTT.SHR > 0) (acceptor-like, if NTT.SHR < 0)
NTT.D	real	0.0	D level density (cm^{-3})
SIG.D	real	0.0	standard deviation (in eV) of gaussian D level distribution
ET.D+ ETL.D+ ETR.D+	real	0.5	D^+ trap level wrt E_V (eV)
ET.D- ETL.D- ETR.D-	real	0.5	D^- trap level wrt E_V (eV)
CP.D-	real	1×10^{-14}	$D^- \rightarrow D^0$ hole capture cross section (cm^2)
CP.D0	real	1×10^{-14}	$D^0 \rightarrow D^+$ hole capture cross section (cm^2)
CN.D+	real	1×10^{-14}	$D^+ \rightarrow D^0$ electron capture cross section (cm^2)
CN.D0	real	1×10^{-14}	$D^0 \rightarrow D^-$ electron capture cross section (cm^2)

LAYER (continued)

Parameter	Type	Default	Description
EG.OPT EGL.OPT EGR.OPT EG2.OPT EG3.OPT	real	-1.	optical bandgap (eV) (-1 sets EG.OPT = EG)
B0.OPT B1.OPT B2.OPT B3.OPT B4.OPT A1.OPT A2.OPT A3.OPT	real real real real real real real real	0.0 0.0 0.0 0.0 0.0 0.0 0.0 0.0	parameters used in optical absorpion calculation (see notes)
TAIL.OPT	logical	FALSE	if TRUE, absorption tail included
ALFC.OPT ZETA.OPT	real real	0.0 0.0	parameters used in absorption tail calculation (see notes)
PH.OPT	logical	FALSE	if TRUE, phonon assisted absorption included
EP1.OPT EP2.OPT ALF.OPT	real real real(6)	0.0 0.0	phonon assisted absorption parameters (see notes)

GENREC

Parameter	Type	Default	Description
RECOMB	char	D	selects recombination mechanisms SHR - single level trap D - D-levels T - band tails
GEN	char	DARK	sets generation rate options- DARK UNIFORM MONO (monochromatic) AM1P5G, etc. (see notes)
WL	real		wavelength for GEN=MONO (μm)
JINC	real	0.1	incident flux ×q (A/cm^2) (GEN=MONO,UNIFORM, or spectral response (SR) option)
CONC	real	1.0	multiplication factor for illumination intensity
SHADOW	real	0.0	relative shadowing factor
GFLAG	integer	0	=0, simple method =1, simple method with dispersion =2, multilayer calculation (see notes)
ANGLE	real	0.0	for GFLAG=0, angle of incidence
RBACK	real	0.0	for GFLAG=0 or =1, relative back surface reflectance
RFRONT	real	0.0	for GFLAG=0 or =1, relative internal front surface reflectance

I-V

Parameter	Type	Default	Description
VSTART	real	0.0	start voltage (V)
VSTOP	real	0.0	stop voltage (V)
DV	real	0.0	voltage increment (V)
V	real( )	0.0	voltage (V)

SOLCELL

Parameter	Type	Default	Description
GFACTOR	integer	10	$10^{-GFACTOR}$ is the initial gereration rate factor for stepping up the intensity
VSTART	real	0.0	start voltage (V)
DVSMALL	real	0.03	smallest voltage increment (V)
DVBIG	real	0.10	largest voltage increment (V)
VSMALL	real	100.	voltage at which DVBIG becomes DVSMALL
RSERIES	real	0.0	external series resistance (Ω–cm^2)
RSHUNT	real	1×10^{51}	external shunt resistance (Ω–cm^2)

SR

Parameter	Type	Default	Description
VA	real	0.0	applied voltage (V)
J(VA)	real	0.0	dark current at V=VA (A/cm^2) (JA(VA) > 0 if VA > 0)
WL	real( )		wavelength (μm) defaults to WL=.34/.36/.38/.40/.44 /.46/.48/.50/.52/.54/.56/.58/.60 /.62/.64/.66/.68/.72/.76

IR

Parameter	Type	Default	Description
JINC	real	0.1	incident flux ×q (A/cm^2)
VA	real	0.0	applied voltage (V)
XMIN	real	0.0	start position for impulse response (μm)
XMAX	real	-1.0	stop position for impulse response (μm) (defaults to device length)
DX	real	-1.0	step size for impulse generation (μm) (defaults to 50 steps)

NOTES

Absorption Model

The absorption coefficient, $\alpha(E)$, is given by

$$\alpha = B0.OPT + B1.OPT\sqrt{E - EG.OPT} + \frac{B2.OPT}{E}(E - EG.OPT)^{1.5} +$$

$$\frac{B3.OPT}{E}(E - EG.OPT)^2 + B4.OPT\,E\,(E - EG.OPT)^2$$

where E is the photon energy in Ev, EG.OPT is the optical bandgap as defined on the LAYER card, and B0.OPT, B1.OPT, B2.OPT, B3.OPT, and B4.OPT are coefficients such that α is in cm^{-1}.

Typical Stoichiometric CuInSe2 Layer Parameters

```
layer  tm=? eg=1.02  ks=13.5 ndx=3.67 nc=6.6e17 nv=1.5e19
+      up=5. un=50. taup.shr=4.4e-9 taun.shr=4.4e-9 et.shr=0.0
+      na=1.e16 eaa=-1.0
+      eg.opt=0.97 eg2.opt=1.10 eg3.opt=2.10
+      a1.opt=5.269631e+04 a2.opt=1.150928e+05 a3.opt=4.518493e+05
+      ph.opt=true ep1.opt=0.031 ep2.opt=0.019
+      alf.opt=5136/2420/1505/1027/873/742
```

Typical Cu_Poor CuInSe2 Layer Parameters (Cu/In/Se = 22.0/26.8/51.2)

```
layer  tm=? eg=1.02  ks=13.5 ndx=3.67 nc=6.6e17 nv=1.5e19
+      up=5. un=50. taup.shr=4.4e-9 taun.shr=4.4e-9 et.shr=0.0
+      na=? eaa=-1.0
+      eg.opt=1.0 eg2.opt=1.105 eg3.opt=0.0
+      a1.opt=5.200364e+04 a2.opt=1.014005e+05 a3.opt=0.0
+      ph.opt=true ep1.opt=0.031 ep2.opt=0.019
+      alf.opt=4228/1733/1282/0.0/0.0/0.0
```

Typical In_Poor CuInSe2 Layer Parameters (Cu/In/Se = 25.7/23.9/50.4)

```
layer  tm=? eg=1.02  ks=13.5 ndx=3.67 nc=6.6e17 nv=1.5e19
+      up=5. un=50. taup.shr=4.4e-9 taun.shr=4.4e-9 et.shr=0.0
+      na=? eaa=-1.0
+      eg.opt=0.96 eg2.opt=1.14 eg3.opt=0.0
+      a1.opt=5.1e4 a2.opt=8.397e4 a3.opt=0.0
+      ph.opt=true ep1.opt=0.031 ep2.opt=0.019
+      alf.opt=6547/5190/4621/3882/3579/3185
```

Plotting of Internal Parameters

Plotting is not supportted with this release. However, T_ADEPTF.EXE (located in the C:\ADEPTF\BIN\ subdirectory) can extract data files containing the desired plot data. These files, consisting of columnar data, can be imported into commercially available plotting packages and spreadsheet programs. to run T_ADEPTF, type

T_ADEPTF *file*. dat

T_ADEPTF is menu driven. A list of internal parameters available for extraction are given in the following table.

PLOTS

Plot	Description
excess	excess carrier concentration
logxcess	log of excess carrier concentration
carrier	carrier concentration
logcar	log of carrier concentration
potent	electrostatic potential
delpot	change from equilibrium of the electrostatic potential
dember	dember potential difference
resist	resistive potential difference
recrate	recombination rate
recomb1	recombination rate (tail & d-level components)
recomb2	recombination rate (b-b and Auger components)
current	current density
efield1	electric field
efield2	electric field
rho	total charge density
rho+rhog	total and gap charge densities
rhotd	tail and dangling bond charge densities
logrhotd	log of the above
rhogap	gap charge density
doping	doping density
eband	energy band diagram
genrate	generation rate
loggen	log of generation rate
mshspace	mesh
mshspac1	mesh
mshspac2	mesh
i-v	current-voltage (xmin, xmax ignored)
iv	current-voltage (xmin, xmax ignored)
sr	spectral response (xmin, xmax ignored)
d-states	d-states vs. energy at xmin, xmax is min. density
t-states	t-states vs. energy at xmin, xmax is min. density

Document Control Page	1. NREL Report No.	2. NTIS Accession No.	3. Recipient's Accession No.
	NREL/TP-413-5092	DE92016444	

4. Title and Subtitle Development of a Computer Model for Polycrystalline Thin-Film $CuInSe_2$ and CdTe Solar Cells	5. Publication Date September 1992 6.
7. Author(s) J.L. Gray, R.J. Schwartz, Y.J. Lee	8. Performing Organization Rept. No.
9. Performing Organization Name and Address School of Electrical Engineering Purdue University West Lafayette, IN 47907	10. Project/Task/Work Unit No. PV231101 11. Contract (C) or Grant (G) No. (C) XN-0-10013-1 (G)
12. Sponsoring Organization Name and Address National Renewable Energy Laboratory 1617 Cole Blvd. Golden, CO 80401-3393	13. Type of Report & Period Covered Technical Report 1 January 1991 - 31 December 1991 14.

15. Supplementary Notes
NREL technical monitor: H.S. Ullal

16. Abstract (Limit: 200 words)

This report describes work to develop an accurate numerical model for $CuInSe_2$ (CIS) and CdTe-based solar cells capable of running on a personal computer. Such a model will aid researchers in designing and analyzing CIS- and CdTe-based solar cells. ADEPT (A Device Emulation Program and Tool) was used as the basis for this model. An additional objective of this research was to use the models developed to analyze the performance of existing and proposed CIS- and CdTe-based solar cells. The development of accurate numerical models for CIS- and CdTe-based solar cells required the compilation of cell performance data (for use in model verification) and the compilation of measurements of material parameters. The development of the numerical models involved implementing the various physical models appropriate to CIS and CdTe, as well as some common window materials. A version of the model capable of running on an IBM-compatible personal computer was developed (primary code development is on a SUN workstation). A user-friendly interface with pop-up menus is continuing to be developed for release with the IBM-compatible model.

17. Document Analysis

a. Descriptors
computer model ; thin films ; copper indium diselenide ; cadmium telluride ; photovoltaics ; solar cells

b. Identifiers/Open-Ended Terms

c. UC Categories
273

18. Availability Statement National Technical Information Service U.S. Department of Commerce 5285 Port Royal Road Springfield, VA 22161	19. No. of Pages 53 20. Price A04

Form No. 0069E (6-30-87)